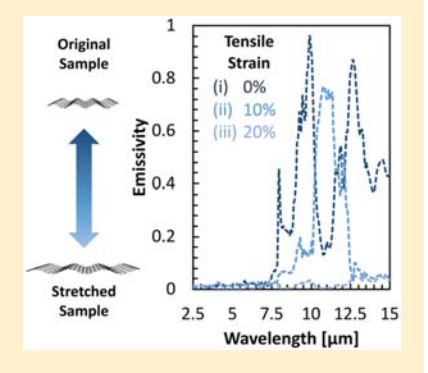


Ultraviolet to Mid-Infrared Emissivity Control by Mechanically Reconfigurable Graphene

Anirudh Krishna, † [5] Jin Myung Kim, ‡ Juyoung Leem, § Michael Cai Wang, §, || SungWoo Nam, *, ‡, § [5] and Jaeho Lee*,

Supporting Information

ABSTRACT: Spectral emissivity control is critical for optical and thermal management in the ambient environment because solar irradiance and atmospheric transmissions occur at distinct wavelength regions. For instance, selective emitters with low emissivity in the solar spectrum but high emissivity in the mid-infrared can lead to significant radiative cooling. Ambient variations require not only spectral control but also a mechanism to adjust the emissivity. However, most selective emitters are fixed to specific wavelength ranges and lack dynamic control mechanisms. Here we show ultraviolet to mid-infrared emissivity control by mechanically reconfiguring graphene, in which stretching and releasing induce dynamic topographic changes. We fabricate crumpled graphene with pitches ranging from 40 nm to 10 μ m using deformable substrates. Our measurements and computations show that 140 nm-pitch crumpled graphene offers ultraviolet emissivity control in 200-300 nm wavelengths whereas 10 μ m-pitch crumpled graphene offers mid-infrared emissivity control in 7–19



μm wavelengths. Significant emissivity changes arise from interference induced by the periodic topography and selective transmissivity reductions. Dynamic stretching and releasing of 140 nm and 10 µm pitch crumpled graphene show reversible emissivity peak changes at 250 nm and at 9.9 μ m wavelengths, respectively. This work demonstrates the unique potential of crumpled graphene as a reconfigurable optical and thermal management platform.

KEYWORDS: Crumpled graphene, selective emitter, selective absorber, metamaterial surface, and radiative cooling

C elective emitters can control the emissivity across distinct regions of the electromagnetic spectrum and allow optimal solutions to systems where a unique wavelength response is desired, which include photonics/optoelectronics, 1,2 infrared (IR) imaging, and thermoregulators.³ In the ambient environment, the solar spectrum exists between the wavelengths of 0.2 and 2.5 μm and can affect the functioning of thermophotovoltaics and systems relying on solar absorption. 4 Meanwhile, the mid-IR wavelength range between 8 and 14 μm (the atmospheric transmission window)⁵ can be utilized for radiative cooling and thermal imaging relying on IR emission.⁶⁻¹¹ Distinct fields of use impose different needs for selective emitters and spectral-selective modulation and control of emissivity by engineered surfaces.

Recent understanding of electromagnetic interactions with artificially engineered microstructures has been making large impacts on the areas of nanophotonics and optoelectronics. There are various emissivity optimization techniques for selective emission/absorption from heterostructure (metallic and semiconductors/oxides) multilayers to photonic structures, gratings, and other architected surface features. ^{7–11} The techniques offered by existing solutions aim to optimize the

emissivity spectra within the atmospheric transmission window from 8 to 14 μ m wavelengths. However, a vast majority of the selective emitters rely on rigid materials and surfaces and have a limited scope of use. The use of flexible materials can offer morphology-controlled¹² dynamic emissivity changes and thus widen the spectral range of use. In general, the solutions offered by passive systems are restricted to particular geographic locations or climatic conditions and would need to be overcome with the use of dynamic systems.

Transient variations in the ambient conditions such as diurnal and seasonal changes and varying environments necessitate dynamic emissivity control. Existing solutions based on phase change materials 13-15 allow emissivity variations that require large temperature excursions and the operations are limited to specific ranges of temperature. Such limitations have been addressed with the use of reconfigurable structures for tunable optical and radiative control. A notable example is the use of stretchable multilayer Bragg stacks that

Received: April 2, 2019 Revised: June 14, 2019 Published: June 28, 2019



Department of Mechanical and Aerospace Engineering, University of California, Irvine, California 92697, United States of America [‡]Department of Materials Science and Engineering and [§]Department of Mechanical Science and Engineering, University of Illinois at Urbana-Champaign, Urbana, Illinois 61801, United States of America

Department of Mechanical Engineering, University of South Florida, Tampa, Florida 33612, United States of America

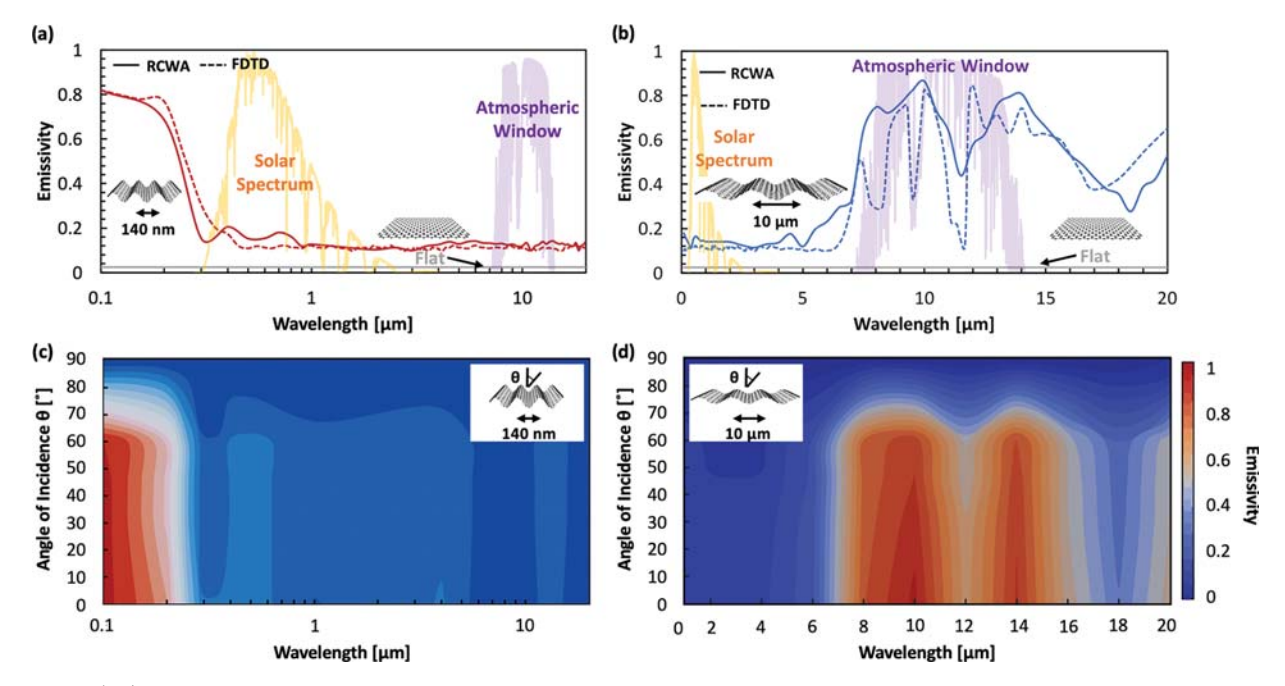


Figure 1. (a,b) Selective emitters based on crumpled graphene. Varying crumpling pitch values affect the radiative cooling and heating opportunities by using the incoming solar radiation⁴ and the atmospheric transmission window.⁵ Comparison of the computed emissivity values of the 140 nm pitch sample and the 10 μ m pitch sample using RCWA and FDTD methods. Emissivity of flat graphene shows a uniformly flat value of 0.025 throughout the spectrum. The profiles are depicted with a focus in the solar and IR regions of the electromagnetic spectrum. (c,d) The solar angle of incidence dependent emissivity spectra for the crumpled graphene of pitch = 140 nm and pitch = 10 μ m, demonstrating the spectrally variant emissivity profiles for a wide range of angles. The color bars indicate surface emissivity values varying from 0 (deep blue) to 1 (deep red). The emissivity profile remains fairly invariant for a majority of the angular range, displaying a sudden decay as the angles approach 90°.

offer tunable IR reflectivity. 16–18 Although several solutions exist for dynamic control of IR properties, such as the use of wave-patterned bimetallic layers that offer strain-induced IR emission control, 19 the use of the Bragg stacks and bimetallic layers only offers control over narrow spectral bands and their reconfigurability is limited due to the use of multilayer structures. There is a distinct lack of fully reconfigurable solutions for ultraviolet (UV) to mid-IR emissivity control. We aim to achieve dynamic modulation of emissivity from the UV to mid-IR wavelengths with the use of a two-dimensional material integrated with a flexible material platform.

Here we present a solution for surface topography-driven emissivity control by crumpled graphene, where periodic undulations in the form of a crumpled structure on the surface of the graphene to control the radiative properties such as emissivity. The choice of graphene is motivated by its demonstrated use for spectral emissivity modulation, and the extremely high in-plane strength, large failure strain, and fatigue resistance of graphene also allow extended lifetime of the proposed crumpled graphene structures.

Optically, flat graphene exhibits a uniformly low emissivity of 0.025 throughout the spectrum $(0.1-20~\mu m)^{.25}$ The spectral emissivity of graphene has been modulated and controlled over the UV to mid-IR spectral ranges so far by electrical modulation 21,22 or nanotexturing. Crumpled graphene, a mechanically self-assembled structure of graphene by stiffness mismatch between graphene and an underlying substrate under mechanical compression, is used in this work to control the spectral emissivity leading to a reconfigurable radiative surface structure. We aim to demonstrate the use of the crumpled graphene with the stretchable material platform to achieve dynamic tunability of emissivity by simple

mechanical straining. From our investigations, we develop an understanding of the relationship of topography and emissivity in the crumpled graphene selective emitters.

Theoretical models using rigorous coupled wave analysis (RCWA) and finite-difference time-domain (FDTD) methods show how the crumpled shapes modulate the surface emissivity profile over the electromagnetic spectrum. The results for RCWA evaluation of crumpled graphene structures depict spectral variation in emissivity profiles for a range of periodic dimensions (Figure 1). The appearance of distinct spectral peaks and dips in the surface emissivity is generally controlled by surface composition, such as material choice, surface thickness and surface morphology. 7,9,12,26 With the material choice and surface thickness remaining the same for all samples presented, the surface emissivity may be controlled primarily by the surface topography.

The crumpled graphene^{27,28} samples consist of a series of periodic slopes with crests and troughs on the surface that are computationally assumed to be the superposition of multiple gratings of different sizes. The interaction of the incident electromagnetic waves with the crumpled surface affects the propagating waves in distinct spectral regions, 12,29,30 leading to changes in the IR and UV/visible (UV/vis) emissivity profiles of different crumpled graphene samples (Figure 1). The emissivity profile for the crumpled graphene samples depends on the interference over adjacent morphological crests. The interference phenomenon leads to spectrally selective emissivity changes. The multiple internal reflection incidents that happen at the graphene surface also induce spectralselective lowering of transmissivity values, dependent on the surface topography and pitch size. The lowering of transmissivity leads to an increase in emissivity over the

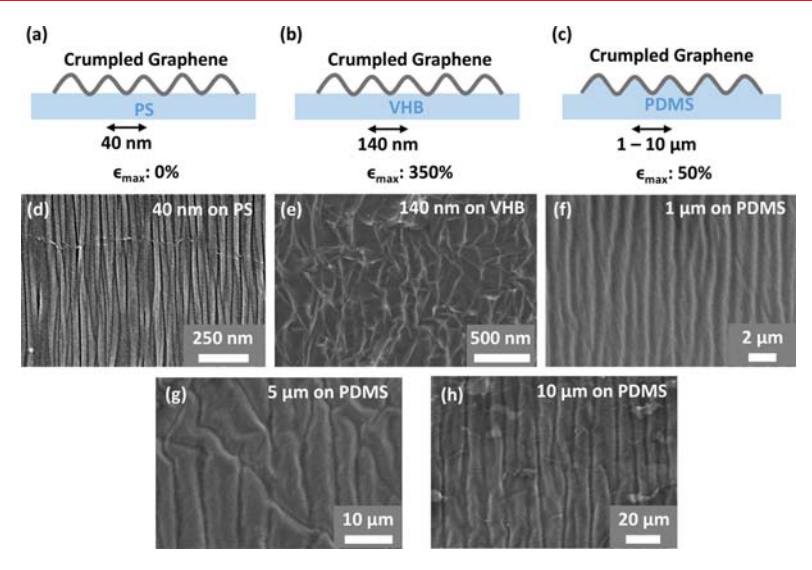


Figure 2. Crumpled graphene has been prepared by allowing a shrinkage of flat graphene on a prestrained polymer substrate, with the maximum possible strain for each substrate denoted by ϵ_{max} (a) Side-view schematic of samples on PS substrate. (b) Side-view schematic of samples on VHB substrate. (c) Side-view schematic of samples on PDMS substrate. The crumpling dimensions ((d) 40 nm, (e) 140 nm, (f) 1 μ m, (g) 5 μ m, (h) 10 μ m) have been characterized by SEM.

topography-controlled spectral regions. In addition to multiple internal reflection, in samples of low pitch sizes (less than 50 nm) the increased emissivity values are also caused by diffraction at the graphene surface due to the undulating crumpled topography.

While multiple underlying phenomena affect the spectral-selective emissivity peaks of the crumpled graphene, we analyzed the predominant factors for each of the samples. For samples of pitch less than 50 nm, diffraction from the undulating surface topography results in an increase in emissivity. The diffraction-dominated variations in spectral emissivity are based on analyses from existing literature on similar samples and related grating structures. For samples of increased pitch, the increase in emissivity due to a reduction in transmissivity is predominantly a result of multiple internal reflection incidents. The wavelength regions corresponding to the reduction in transmissivity are determined by interference phenomena corresponding to the crumpled graphene pitch.

The emissivity spectra of crumpled graphene can be tuned by controlling the pitch, which acts as the predominant geometric parameter apart from the crumpling amplitude (Figure S1). The rise and fall in the high emissivity region are controlled by the crumpling pitch owing to the interference of photons over multiple adjacent crests and the shifting of the spectral region dominated by diffraction. With an increase in the pitch, the beginning of the spectral region dominated by the diffraction-induced peaks is shifted to longer wavelengths (Figure S2). This moves the high emissivity region further toward the IR as we increase the pitch. Increasing the pitch size of the crumpled graphene also narrows the high emissivity region (Figure S1b). Decreasing the pitch leads to a loss in spectral-selective emissivity characteristics, leading to the emissivity profile approaching a spectrally flat one (Figure S1b). For crumpled graphene samples with a pitch size of 140 nm, the emissivity spectrum shows high emissivity within the UV spectrum. For an increased pitch size of 10 μ m, the results indicate high emissivity in the mid-IR wavelengths (Figure 1a,b). Although changes in pitch dictate spectral variations in

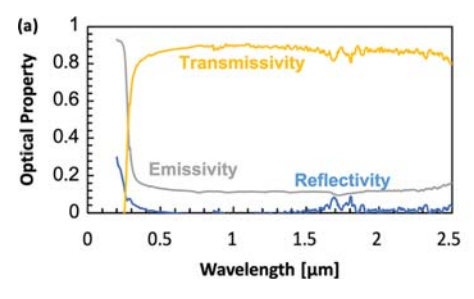
emissivity, changes in aspect ratio (crumple height/pitch) from 0.2 to 1 do not lead to significant variations in emissivity (Figure S1c).

These spectral emissivity results also depend on the solar zenith angles of incidence, and the crumpled graphene design may be optimized depending on the device and environmental conditions. The emissivity profile of the crumpled graphene as a function of solar angle of incidence (Figure 1c,d) indicates a largely angle-independent profile that shows a steep decay in spectral characteristics with large angles of incidence beyond 70°. This is consequently helpful for the use of crumpled graphene structures in vast areas of the earth, with most high-population centers laying in areas of relatively low solar angle of incidence regions.

We have fabricated and characterized surface corrugations of graphene in pitch sizes of 40 nm to 10 μ m²⁹ (Figure 2). The crumpled graphene of the lower pitch sizes (40 to 140 nm) were fabricated on either a polystyrene (PS) or a very high bond (VHB) substrate, whereas the samples of higher pitch size (1–10 μ m) were fabricated on a poly(dimethylsiloxane) (PDMS) substrate.

Chemical vapor deposition (CVD) grown graphene was used for sample preparation. The detailed recipe of graphene growth is described in previous publications. ^{20,33,34} Prestrained, shape memory polymer (prestrained polystyrene) substrate was used for 40 nm pitch samples. The highly stretchable elastomeric substrate was stretched with prestrain of 350% for 140 nm pitch samples. Graphene on copper foil was gently attached onto the prestrained or prestretched substrate, and sodium persulfate (Na₂S₂O₈, purchased from Sigma-Aldrich, MA) aqueous solution was loaded on it to etch copper foil. After the copper foil is completely dissolved, the applied prestrains are slowly and steadily removed from the substrate. Because of the strain mismatch and elasticity difference, the graphene layer is buckled and delaminated from the underlaying substrate, and it forms a crumpled structure.

The poly(dimethylsiloxane) (PDMS) substrate was prepared by mixing the prepolymer and the cross-linking agent



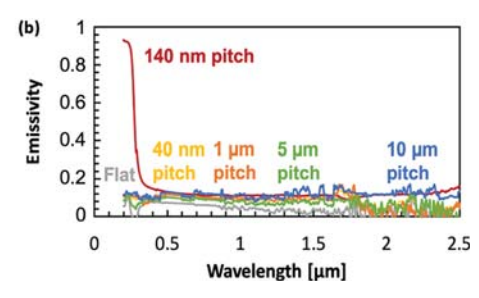
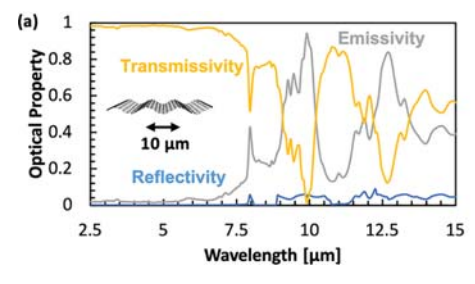


Figure 3. (a) Optical measurements of crumpled graphene of 140 nm pitch using UV/vis spectroscopy. (b) UV/vis spectroscopy results for the emissivity of flat graphene, showing an emissivity value of 0.025, which agrees with the literature value, 140 nm pitch crumpled graphene showing an emissivity peak dropping off at 250–300 nm wavelength, and 40 nm, 1 μ m, 5 μ m, and 10 μ m pitch crumpled graphene depicting uniformly flat emissivity profiles.



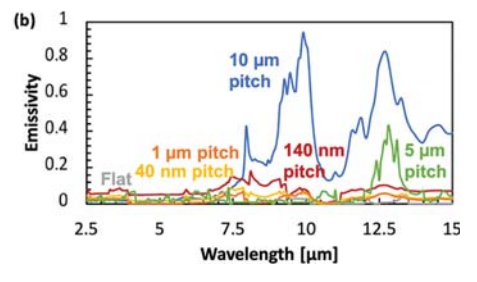


Figure 4. (a) Optical measurements of crumpled graphene of 10 μ m pitch using FTIR spectroscopy. (b) FTIR spectroscopy results for the emissivity of flat graphene, showing a uniformly low emissivity value, 40 nm, 140 nm, 1 μ m, and 5 μ m pitch crumpled graphene showing low emissivity profiles, although slightly above flat graphene values, and 10 μ m pitch crumpled graphene depicting emissivity peaks (and transmissivity dips) from 8 to 14 μ m wavelength.

(Sylgard 184, Dow Corning incorporation) and subsequently curing the mixture at 70 °C for 60 min. The prepared substrate was uniaxially stretched with prestrain of 20%, and then treated with CHF₃ reactive ion etching (RIE) at a power of 90 W and a flow rate of 30 sccm under 100 mTorr of chamber pressure in order to deposit a fluorocarbon (CF_x) skin layer.³⁵ The wrinkle pitch was determined by RIE treatment time varying 4, 17, and 35 min for 1, 5, and 10 μ m pitch, respectively. CVD-grown graphene was spin-coated with poly(methyl methacrylate) (PMMA) (950 PMMA A2, Microchem) and floated on top of sodium persulfate solution until the underlying copper is removed. Afterward, PMMA/graphene was transferred to the CF_x /PDMS substrate, and PMMA was dissolved in acetone. The final wrinkle structure of graphene/PDMS was obtained by releasing prestrain slowly.

The corrugation pitch sizes of the samples were verified using scanning electron microscopy (SEM) imaging, and the SEM images show samples of pitch sizes varying from 40 nm to 10 μ m (Figure 2). The samples were then evaluated using UV/vis and Fourier transform infrared (FTIR) spectroscopy to obtain emissivity results from 200 nm to 15 μ m wavelength.

The spectrometric analyses of the crumpled graphene samples in the UV/vis spectral range were carried out using UV/vis spectroscopy from 200 nm up to 2.5 μ m wavelength (Figure 3). The emissivity, for all spectrmetric analyses, is recorded as unity minus the sum of the transmissivity and refelctivity, with the emissivity being assumed equal to the absorptivity. The spectrometric data was taken as a differential measurement with the polymer substrate taken as the baseline data from which the sample (crumpled graphene) was recorded as the measured data. This results in spectrometric results purely for the crumpled graphene structures, eliminating the substrates underneath. While the flat graphene

measurement shows a uniformly flat, low emissivity profile of 0.02–0.05, the crumpled graphene samples depict spectral variations in the emissivity profiles. In the UV/vis wavelengths, the 140 nm pitch sample demonstrates an emissivity peak dropping off at 250–300 nm, which is diminished with an increase in crumpling pitch (as demonstrated by the near flat UV/vis profile of the 10 μ m pitch sample) (Figure 3b). Variations in the pitch around the mean value for the 140 nm pitch crumpled graphene are predicted to have minimal effect in the spectral emissivity profile, based on RCWA computations (Figures S3 and S5).

The spectrometric analyses of the crumpled graphene samples in the mid-IR spectral range were carried out using FTIR spectroscopy beyond 2.5 μ m wavelength (Figure 4). The spectra were taken as a differential measurement normalized against the polymer substrate to record purely the measurements from the crumpled graphene structures. In the mid-IR wavelengths, we notice a prominent emissivity peak in the 8-14 μ m spectral region for the 10 μ m pitch sample, which shows a gradual appearance upon increasing the pitch. This peak is absent in the low (140 nm) pitch sample (Figure 4b). The emissivity variations are a result of multiple diffraction and interference phenomena among adjacent crumple features and behave as evidenced by the simulation results shown in Figure 1. Variations in the pitch around the mean value for the 10 μ m pitch crumpled graphene are predicted to have minimal effect in the spectral emissivity profile, based on RCWA computations (Figure S4 and S5). The pitch-dependent emissivity variations are also accompanied by changes to other optical properties, such as complex refractive index (Figure S6).

All crumpled graphene samples, irrespective of crumple pitches, are expected to depict spectral-selective emissivity

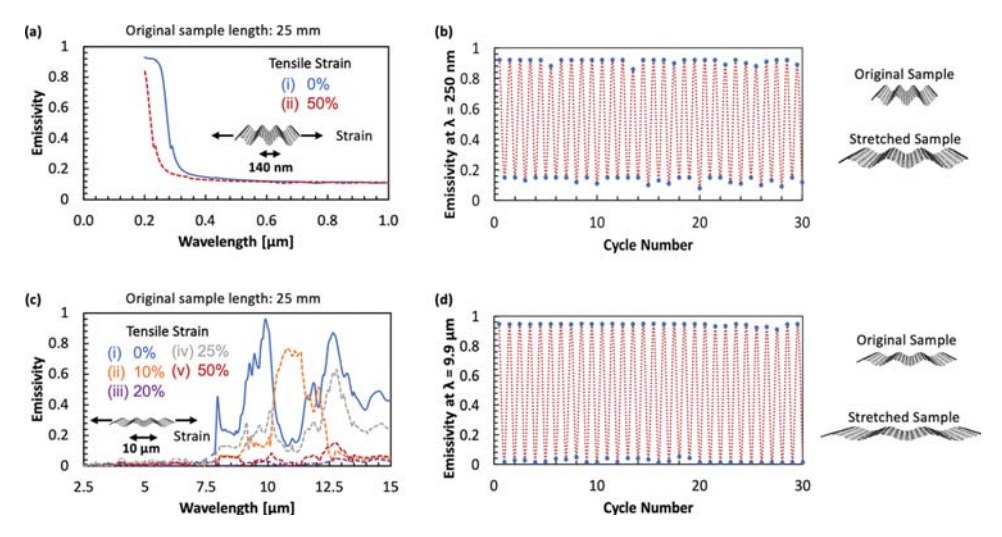


Figure 5. Experimental demonstration of reconfigurable graphene systems for dynamic emissivity control. (a) By gently straining the 140 nm pitch crumpled graphene, the drop in the emissivity spectrum has blue-shifted, corresponding to a change in the pitch. (b) Emissivity measurements for 140 nm pitch crumpled graphene over 30 cycles of stretching and relaxation, at a wavelength of $0.25 \mu m$ show a retention of its characteristics. (c) By straining the 10 μm pitch crumpled graphene sample, the corresponding change in crumpling pitch has lessened the peaks in emissivity with further peaks appearing with increased tensile strain due to transverse crumpling. (d) Emissivity measurements for 10 μm pitch crumpled graphene over 30 cycles of stretching and relaxation at a wavelength of 9.9 μm show a retention of its characteristics over multiple cycles of stretching.

profiles (Figure S1). Although the 140 nm and 10 μ m pitch crumpled graphene samples are considered for further analysis in the UV/visible and IR wavelength regions, they do not represent unique cases. The 1 μ m pitch crumpled graphene is predicted to exhibit emissivity peaks between the wavelengths of 6–12.5 μ m. Similarly, computations and measurements for the 5 μ m pitch crumpled graphene exhibit an emissivity peak between the wavelengths of 12–15 μ m (Figure 4b).

A major advantage of the mechanically induced nature of surface corrugations in graphene is the ability to allow shape reconfiguration. To explore the mechanical reconfigurability of crumpled graphene structures on elastomeric substrates, we have carried out key characterizations of crumpled graphene (i.e., optical measurements in the visible and IR wavelength range) as mechanical strain is applied.

The reconfigurability of the crumpling effect on emissivity has been demonstrated on a stretchable polymer substrate by characterizing the measured spectra before and after stretching the substrate (Figure 5a,b). The emissivity of stretched (reflattened) crumpled graphene is lowered as we stretched the structure, but it was still higher than emissivity of flat graphene sample which was prepared on an unstrained bare polymer substrate. The flat graphene samples show a very low emissivity throughout the spectrum, as indicated in earlier studies. ²⁵

In Figure 3b, the crumpled graphene samples of 140 nm pitch, prepared by a substrate shrinkage, show a very low emissivity in the near IR range. By applying tensile strain to the crumpled graphene samples (Figure 5a), there is a reduction in the emissivity values for the wavelength range below 300 nm owing to the flattening of the graphene crumples. A greater change in the emissivity spectrum, closer to the full recovery of the flat graphene data, is expected by fully flattening the graphene via increased strain. The presented data sets show the possibility of developing a mechanically reconfigurable optical system based on crumpled graphene.

Our results (Figure 5b) also demonstrate consistent emissivity tunability over multiple cycles of stretching and

relaxation. The Figure 5b depicts the spectral emissivity value taken at a wavelength of 0.25 μ m over 30 cycles of stretching and relaxation for a crumpled graphene sample with an original pitch of 140 nm. Tensile straining the substrate increases the crumpled graphene pitch and the corresponding blueshift leads to the originally emissive sample losing its emissive nature (at a wavelength of 0.25 μ m). With each cycle, the stretching and relaxation lead to an on–off behavior for the crumpled graphene. The samples do not display changes in emissivity values related to fatigue over multiple cycles of measurement and may withstand further cycles of testing without significant loss in spectral emissivity values.

Similarly, the reconfigurability tests were performed on the 10 μ m pitch sample to quantify the data in the IR regions (Figures 5c, 5d). The measured emissivity peak (and corresponding transmissivity dip) in the mid-IR wavelengths shows a loss in spectral variations with increased strain due to the increase in crumpling pitch posed by mechanical stretching normal to the crumple axis. The sample was stretched to varying levels of applied strain, and shows a stepwise loss in spectral properties. The dip in spectral emissivity in the mid-IR regions was likely caused by the increase in pitch sizes due to the mechanical straining of the substrate. Our computational fitting parameters suggest that the modulated pitch for the crumpled graphene samples (Figure 5c) with increasing tensile strain range from 12 to 15 μ m.

The 10 μ m pitch samples were also subjected to tensile strains beyond the original prestrain condition of 20%. Characterizing the emissivity profiles for the samples when subjected to tensile strains of 0%, 10%, 20%, 25%, and 50% (Figure 5c), the emissivity peak for the samples shifts from a wavelength of around 10 μ m for a strain of 0%, to a wavelength of around 11 μ m for a strain of 10%. When the strain is increased to 20%, the emissivity profile flattens out and has no discernible peak. With a further increase in strain to 25% and beyond, emissivity peaks appear in longer wavelengths, perhaps due to the transverse crumples or the formation of cracks. The samples showed negligible deterioration in spectral

emissivity characteristics upon return to original state after being subjected to such increased strain, even over multiple cycles (Figure S7), demonstrating the reconfigurability of the crumpled graphene samples.

The spectral emissivity measurements for the 10 μ m pitch samples were also recorded as cyclical data (Figure 5d) with the measurements at a wavelength of 9.9 μ m (which recorded the spectral peak emissivity) depicting an on–off behavior in spectral emissivity. By using a two-way (multistate) shape memory substrate or a mechanically actuatable soft substrate, these surface corrugations can be readily tuned to different topographies spanning 100 nm to 100 μ m.

The tunable emissivity modulated by mechanically controlled crumpling of graphene enables novel dynamic temperature control systems. On the basis of the surface topographies of graphene and the selective surface emission with respect to the solar spectrum and the mid-IR ranges, the surface temperature can be dynamically controlled depending on the application. The spectral emissivity of crumpled graphene samples of varying pitch sizes is first computed using RCWA and FDTD simulations. The spectral emissivity is then used to compute the net radiative power and surface temperature using eq S1.

To predict the impact of crumpled graphene surfaces in normal ambient conditions, considerable heat transfer by convection and conduction (i.e., $h_{eq} = 10 \text{ W m}^{-2} \text{ K}^{-1}$) are assumed with transient solar irradiance under clear sky. 12 The ambient conditions are taken to be average values for California with the ambient temperature varying between 286 and 300 K through the day. The solar zenith angle of incidence is also assumed to be the value taken in California³ with the average angle being 30°. The computation shows that the crumpled graphene of 10 μm pitch size can achieve a net cooling power of 77 W m⁻² at an ambient temperature of 300 K and a surface temperature reduction 7 K below the ambient air (Figure S8). The predicted tunable temperature range is shown to be 10 K in the normal ambient conditions (and up to 80 K in the theoretical limit of a completely isolated system). The crumpled graphene may lead to tunable subambient radiative cooling (with the 10 μ m pitch crumpled graphene) or above ambient heating (with the 140 nm pitch crumpled graphene).

The use of large pitch ($10~\mu m$) crumpled graphene can offer visible transparency (with a transmissivity >0.8) while allowing for IR emissivity control with potential implications for IR sensing and thermal imaging sensitive to the wavelengths of 8–14 μm . Similarly, the visible-transparent, UV-opaque (transmissivity <0.1) behavior of the small pitch (140 nm) crumpled graphene could affect materials and surfaces sensitive to the strong solar UV irradiation up to 300 nm wavelength. The flexible nature of the crumpled graphene also makes it a suitable candidate for use in wearable systems where radiative cooling could have a big impact in the performance of systems.

This study provides a fundamental understanding of the relationship between topography and emissivity for crumpled graphene and demonstrates a mechanically reconfigurable optical and thermal management platform. Computations based on spectral emissivity using the RCWA and FDTD methods guide optimal designs of dynamic selective emitters. Measurements based on UV/vis and FTIR spectroscopies validate the emissivity of crumpled graphene samples with varying pitch sizes. The small pitch (140 nm) crumpled graphene offers emissivity control ranging in the UV

wavelengths with a high emissivity greater than 0.8 up to a wavelength of 300 nm. The large pitch (10 μ m) crumpled graphene offers control over the mid-IR wavelengths with a high emissivity greater than 0.6 in the mid-IR region between 7 and 19 μ m.

The integration of crumpled graphene with stretchable polymer substrates facilitates mechanical reconfigurability of the emitter. The topography changes associated with the strain induce corresponding emissivity variations. As the tensile strain increases to 50% on the 140 nm pitch sample, the emissivity peak shifts from 250 to 200 nm. Similarly, an increased tensile strain on the 10 μ m sample shifts the emissivity to higher wavelengths and simultaneously narrows the emissivity peak. These changes are reversible over multiple cycles and demonstrate a reconfigurable tunable emissivity structure.

While most existing solutions offer passive emissivity control, the results presented here demonstrate the possibility of dynamic spectral emissivity control with crumpled graphene structures. The analytical modeling of net heat flux and surface temperature demonstrates the possibilities of developing a dynamic thermal control system and achieving above ambient heating and subambient cooling based on the spectral emissivity control offered by the crumpled graphene. This mechanically reconfigurable graphene has implications for systems that could range from IR sensors and bolometers to thermoregulators. The use of the crumpled graphene selective emitters deepens our understanding of dynamic optical control and enables new optical and thermal technologies.

ASSOCIATED CONTENT

Supporting Information

The Supporting Information is available free of charge on the ACS Publications website at DOI: 10.1021/acs.nanolett.9b01358.

Crumpling pitch-dependent spectral emissivity computation, spectroscopy measurements, cyclical straining of $10~\mu m$ pitch crumpled graphene, and thermal energy balance in the ambient environment (PDF)

AUTHOR INFORMATION

Corresponding Authors

*E-mail (S.W.N.) swnam@illinois.edu. *E-mail: (J.L.) jaeholee@uci.edu.

ORCID ®

Anirudh Krishna: 0000-0002-5619-1569 SungWoo Nam: 0000-0002-9719-7203

Notes

The authors declare no competing financial interest.

ACKNOWLEDGMENTS

A.K. and J.L. thank the support from the Henry Samueli School of Engineering at the University of California, Irvine and the Hellman Faculty Award. A.K. would like to thank the training provided by Dr. Qiyin Lin at the UC Irvine Materials Research Institute and Dr. Dmitry Fishman at the UC Irvine Laser Spectroscopy Lab. S.N. gratefully acknowledges support from the AFOSR (FA9550-16-1-0251 and FA2386-17-1-4071), NSF (MRSEC DMR-1720633 and CMMI-1554019), ONR (N00014-17-1-2830) and NASA ECF (NNX16AR56G). This research was partially supported by the NSF through the

University of Illinois at Urbana-Champaign Materials Research Science and Engineering Center DMR-1720633.

REFERENCES

- (1) Lenert, A.; Bierman, D. M.; Nam, Y.; Chan, W. R.; Celanović, I.; Soljačić, M.; Wang, E. N. A nanophotonic solar thermophotovoltaic device. *Nat. Nanotechnol.* **2014**, *9*, 126–130.
- (2) Hu, L.; Chen, G. Analysis of optical absorption in silicon nanowire arrays for photovoltaic applications. *Nano Lett.* **2007**, *7*, 3249–52.
- (3) Quintiere, J. Radiative characteristics of fire fighters' coat fabrics. *Fire Technol.* **1974**, *10*, 153–161.
- (4) Gueymard, C. A.; Myers, D.; Emery, K. Proposed reference irradiance spectra for solar energy systems testing. *Sol. Energy* **2002**, 73, 443–467.
- (5) Lord, S. D. A New Software Tool for Computing Earth's Atmospheric Transmission of Near- and Far-Infrared Radiation; NASA Technical Memorandum 103957; NASA, 1992.
- (6) Catalanotti, S.; Cuomo, V.; Piro, G.; Ruggi, D.; Silvestrini, V.; Troise, G. The radiative cooling of selective surfaces. *Sol. Energy* **1975**, 17, 83–89.
- (7) Raman, A. P.; Anoma, M. A.; Zhu, L.; Rephaeli, E.; Fan, S. Passive radiative cooling below ambient air temperature under direct sunlight. *Nature* **2014**, *515*, 540–544.
- (8) Chen, Z.; Zhu, L.; Raman, A.; Fan, S. Radiative cooling to deep sub-freezing temperatures through a 24-h day—night cycle. *Nat. Commun.* **2016**, *7*, 13729.
- (9) Kou, J.; Jurado, Z.; Chen, Z.; Fan, S.; Minnich, A. J. Daytime radiative cooling using near-black infrared emitters. *ACS Photonics* **2017**, *4*, 626–630.
- (10) Zhai, Y.; Ma, Y.; David, S. N.; Zhao, D.; Lou, R.; Tan, G.; Yang, R.; Yin, X. Scalable-manufactured randomized glass-polymer hybrid metamaterial for daytime radiative cooling. *Science* **2017**, 355, 1062–1066
- (11) Huang, Z.; Ruan, X. Nanoparticle embedded double-layer coating for daytime radiative cooling. *Int. J. Heat Mass Transfer* **2017**, 104. 890–896.
- (12) Krishna, A.; Lee, J. Morphology-Driven Emissivity of Microscale Tree-like Structures for Radiative Thermal Management. *Nanoscale Microscale Thermophys. Eng.* **2018**, 22, 124–136.
- (13) Ono, M.; Chen, K.; Li, W.; Fan, S. Self-adaptive radiative cooling based on phase change materials. *Opt. Express* **2018**, 26, A777–A787.
- (14) Wang, H.; Yang, Y.; Wang, L. Switchable wavelength-selective and diffuse metamaterial absorber/emitter with a phase transition spacer layer. *Appl. Phys. Lett.* **2014**, *105*, 071907.
- (15) Taylor, S.; Yang, Y.; Wang, L. Vanadium dioxide based Fabry-Perot emitter for dynamic radiative cooling applications. *J. Quant. Spectrosc. Radiat. Transfer* **2017**, *197*, 76–83.
- (16) Phan, L.; Walkup IV, W. G.; Ordinario, D. D.; Karshalev, E.; Jocson, J. M.; Burke, A. M.; Gorodetsky, A. A. Reconfigurable infrared camouflage coatings from a cephalopod protein. *Adv. Mater.* **2013**, 25, 5621–5625.
- (17) Kolle, M.; Lee, S. Progress and Opportunities in Soft Photonics and Biologically Inspired Optics. *Adv. Mater.* **2018**, *30*, 071907.
- (18) Xu, C.; Stiubianu, G. T.; Gorodetsky, A. A. Adaptive infrared-reflecting systems inspired by cephalopods. *Science* **2018**, 359, 1495–1500.
- (19) Kazemi Moridani, A.; Zando, R.; Xie, W.; Howell, I.; Watkins, J. J.; Lee, J. H. Plasmonic Thermal Emitters for Dynamically Tunable Infrared Radiation. *Adv. Opt. Mater.* **2017**, *5*, 1600993.
- (20) Wang, M. C.; Chun, S.; Han, R. S.; Ashraf, A.; Kang, P.; Nam, S. Heterogeneous, three-dimensional texturing of graphene. *Nano Lett.* **2015**, *15*, 1829–1835.
- (21) Brar, V. W.; Sherrott, M. C.; Jang, M. S.; Kim, S.; Kim, L.; Choi, M.; Sweatlock, L. A.; Atwater, H. A. Electronic modulation of infrared radiation in graphene plasmonic resonators. *Nat. Commun.* **2015**, *6*, 7032.

(22) Salihoglu, O.; Uzlu, H. B.; Yakar, O.; Aas, S.; Balci, O.; Kakenov, N.; Balci, S.; Olcum, S.; Süzer, S.; Kocabas, C. Graphene-Based Adaptive Thermal Camouflage. *Nano Lett.* **2018**, *18*, 4541–4548

- (23) Anguita, J. V.; Ahmad, M.; Haq, S.; Allam, J.; Silva, S. R. P. Nanotechnology: Ultra-broadband light trapping using nanotextured decoupled graphene multilayers. *Sci. Adv.* **2016**, *2*, e1501238.
- (24) Lee, C.; Wei, X.; Kysar, J. W.; Hone, J. Measurement of the elastic properties and intrinsic strength of monolayer graphene. *Science* **2008**, 321, 385–388.
- (25) Muley, S. V.; Ravindra, N. M. Emissivity of electronic materials, coatings, and structures. *JOM* **2014**, *66*, 616–636.
- (26) Smith, G.; Gentle, A.; Arnold, M.; Cortie, M. Nanophotonics-enabled smart windows, buildings and wearables. *Nanophotonics* **2016**, 5, 55–73.
- (27) Weber, J. W.; Calado, V. E.; Van De Sanden, M. C. M. Optical constants of graphene measured by spectroscopic ellipsometry. *Appl. Phys. Lett.* **2010**, 97, 091904.
- (28) Ochoa-Martínez, E.; Gabás, M.; Barrutia, L.; Pesquera, A.; Centeno, A.; Palanco, S.; Zurutuza, A.; Algora, C. Determination of a refractive index and an extinction coefficient of standard production of CVD-graphene. *Nanoscale* **2015**, *7*, 1491–1500.
- (29) Magnusson, R.; Gaylord, T. K. Analysis of multiwave diffraction of thick gratings. *J. Opt. Soc. Am.* **1977**, *67*, 1165.
- (30) Moharam, M. G.; Gaylord, T. K. Rigorous coupled-wave analysis of planar-grating diffraction. J. Opt. Soc. Am. 1981, 71, 811.
- (31) Moharam, M. G. Coupled-Wave Analysis Of Two-Dimensional Dielectric Gratings. In *Holographic Optics: Design and Applications*; International Society for Optics and Photonics, 1988; Vol. 883, p 8.
- (32) Sala-Casanovas, M.; Krishna, A.; Yu, Z.; Lee, J. Bio-Inspired Stretchable Selective Emitters Based on Corrugated Nickel for Personal Thermal Management. *Nanoscale Microscale Thermophys. Eng.* **2019**, 23, 173.
- (33) Kang, P.; Wang, M. C.; Knapp, P. M.; Nam, S. Crumpled Graphene Photodetector with Enhanced, Strain-Tunable, and Wavelength-Selective Photoresponsivity. *Adv. Mater.* **2016**, *28*, 4639–4645.
- (34) Leem, J.; Wang, M. C.; Kang, P.; Nam, S. Mechanically Self-Assembled, Three-Dimensional Graphene-Gold Hybrid Nanostructures for Advanced Nanoplasmonic Sensors. *Nano Lett.* **2015**, *15*, 7684–7690.
- (35) Rhee, D.; Lee, W. K.; Odom, T. W. Crack-Free, Soft Wrinkles Enable Switchable Anisotropic Wetting. *Angew. Chem., Int. Ed.* **2017**, 56, 6523–6527.
- (36) U.S. Department of Commerce, NOAA, E. S. R. L. ESRL Global Monitoring Division Global Radiation Group; https://www.esrl.noaa.gov/gmd/grad/stardata.html.